Self-consistent approach to many-body localization and subdiffusion

P. Prelovšek[1,2] and J. Herbrych[3,4]
[1]*Jožef Stefan Institute, SI-1000 Ljubljana, Slovenia*
[2]*Faculty of Mathematics and Physics, University of Ljubljana, SI-1000 Ljubljana, Slovenia*
[3]*Department of Physics and Astronomy, The University of Tennessee, Knoxville, Tennessee 37996, USA*
[4]*Materials Science and Technology Division, Oak Ridge National Laboratory, Oak Ridge, Tennessee 37831, USA*
(Received 18 September 2016; revised manuscript received 10 May 2017; published 17 July 2017)

An analytical theory, based on the perturbative treatment of the disorder and extended into a self-consistent set of equations for the dynamical density correlations, is developed and applied to the prototype one-dimensional model of many-body localization. Results show a qualitative agreement with the numerically obtained dynamical structure factor in the whole range of frequencies and wave vectors, as well as across the transition to nonergodic behavior. The theory reveals the singular nature of the one-dimensional problem, whereby on the ergodic side the dynamics is subdiffusive with dynamical conductivity $\sigma(\omega) \propto |\omega|^{\alpha}$, i.e., with vanishing dc limit $\sigma_0 = 0$ and $\alpha < 1$ varying with disorder, while we get $\alpha > 1$ in the localized phase.

DOI: 10.1103/PhysRevB.96.035130

I. INTRODUCTION

Many-body localization (MBL) is a challenging phenomenon involving the interplay of disorder and particle interaction (correlations). In the fermionic systems it has been proposed as an extension of the single-particle Anderson localization [1,2], remaining qualitatively valid at finite interactions [3,4] and at large enough disorder even at high temperature T [5]. In contrast to normal (ergodic) systems, the MBL state should reveal vanishing dc transport [6–12] as well as a nonergodic time evolution of correlation functions and of quenched initial states [13–20]. The vanishing of dc mobility [21] and the nonergodic decay of the initial density profile [22–24] have been the main experimental signatures of the MBL in fermionic cold-atom systems.

The dynamical structure factor $S(q,\omega)$ is the obvious observable to characterize the one-dimensional (1D) system undergoing the ergodic-nonergodic (MBL) transition. Theoretical studies so far concentrated mostly on the uniform (wave vector $q \to 0$) response, e.g., as contained in the optical conductivity $\sigma(\omega)$ and its dc limit σ_0 [6–12]. In this connection, a challenging question is the possibility of subdiffusive dynamics [8,9,24–28], which implies vanishing dc transport, e.g., $\sigma_0 = 0$, but anomalous low-ω dependence of the optical conductivity $\sigma \propto |\omega|^{\alpha}$ with $\alpha < 1$. On the other hand, in the cold-atom experiments so far more accessible are density correlations with $q = \pi$ [22,29,30], as measured via the time-dependent imbalance [22–24].

In this paper we first present results for $S(q,\omega)$ within the prototype disordered 1D model of interacting spinless fermions, displaying the whole range of wave vectors $q = [0,\pi]$, as obtained with a numerical calculation at $T \to \infty$ on small finite-size systems with up to $L = 24$ sites. We show that it is convenient and informative to analyze the $S(q,\omega)$ spectra in terms of memory functions, representing the corresponding dynamical conductivity $\sigma(q,\omega)$ and even further, the current-decay-rate function $\Gamma(q,\omega)$. Such quantities reveal more clearly the transition to the MBL regime, as well as the behavior in the case of subdiffusion.

We further introduce for the same model an analytical theory based on the perturbative treatment of the current-decay function $\Gamma(q,\omega)$ and extended to a self-consistent (SC) evaluation of density-correlation function $\phi(q,\omega)$. The theory reveals the specific nature of the 1D problem, leading to a singular coupling between $q \to 0$ density and energy diffusion modes. Still, the solution of the SC equations with an additional cutoff simulating a finite system size L^* shows qualitative (and at weaker disorder even quantitative) agreement with numerically obtained results for $S(q,\omega)$ and related $\sigma(q,\omega)$. Moreover, the finite-size scaling of SC results reveals in the ergodic phase the subdiffusive dynamics, consistent with $\sigma(\omega \to 0) \approx |\omega|^{\alpha}$ with $\alpha < 1$. The MBL transition at critical disorder $W = W_c$ is thus determined by a dynamical exponent $\alpha = 1$, while the MBL phase is characterized by $\alpha > 1$ and a finite dielectric polarizability $\chi_{\rm d}$ of the insulating system.

The paper is organized as follows: In Sec. II we present the model and the general formalism for density dynamical susceptibility $\chi(q,\omega)$, which is related to generalized dynamical conductivity $\sigma(q,\omega)$ and further to the current-decay-rate function $\Gamma(q,\omega)$. In Sec. III we present results for $S(q,\omega)$, obtained via the numerical exact-diagonalization technique for $T \to \infty$ on finite chains for all available q. Results of $\sigma(q,\omega)$ and $\Gamma(q,\omega)$, obtained with help of formalism introduced in Sec. II, are also presented. This allows for connection with previous studies of, e.g., optical conductivity $\sigma(\omega)$ and also motivation as well as a stringent test for the proposed analytical theory. In Sec. IV we introduce analytical approximations, based on the perturbative treatment of $\Gamma(q,\omega)$. Furthermore, with some additional simplifications, the solution for $\Gamma(q,\omega)$ is extended into a SC set of equations. Numerical results of these equations are presented and commented on in Sec. V. Besides the qualitative agreement with finite-size results, we put the emphasis on the low-ω regime where the SC equations appear to be singular in 1D. Scaling an effective chain length L^* we show that in the ergodic regime the solutions are consistent with an interpretation in terms of a subdiffusion phenomenon. Conclusions, critical reflections on the method, and results are given in Sec. VI.

II. DYNAMICAL DENSITY CORRELATIONS

We consider the prototype (standard) model of MBL, the 1D system of interacting spinless fermions with random local

potentials,

$$H = -t\sum_i (c^\dagger_{i+1}c_i + \text{H.c.}) + V\sum_i n_{i+1}n_i + \sum_i \epsilon_i n_i. \tag{1}$$

As usual, we assume quenched disorder with the uniform distribution $-W < \epsilon_i < W$ and in the numerical analysis the system at half-filling, i.e., $\bar{n} = 1/2$. We further-on use $t = 1$ as the unit of energy. While most numerical results so far are for $V = 2$ (corresponding to the isotropic Heisenberg model [6,8–12]), we use for the demonstration $V = 1$, enabling closer comparison with the analytical theory. Since T should not play an essential role in the MBL problem, studies are adapted to the limit $\beta = 1/T \to 0$, which simplifies the analytical as well as the numerical approach.

Our analysis deals with dynamics of the density operator

$$n_q = \frac{1}{\sqrt{L}}\sum_i e^{\imath qi} n_i, \tag{2}$$

at arbitrary wave vector q, as defined by the dynamical susceptibility $\chi(q,\omega)$ and the related relaxation function $\phi(q,\omega)$,

$$\chi(q,\omega) = \imath\int_0^\infty d\tau\, e^{\imath\omega\tau}\langle[n_q(\tau),n_{-q}]\rangle,$$
$$\phi(q,\omega) = \frac{1}{\omega}[\chi(q,\omega) - \chi^0(q)], \tag{3}$$

with its static (thermodynamic) value $\chi^0(q)$ (see formal background and definitions in Appendix A), which in normal ergodic systems satisfies $\chi^0(q) = \chi(q,\omega \to 0)$.

In a homogeneous system $\langle..\rangle$ denotes the canonical thermodynamical average. In a disordered system we perform in addition the averaging over all random configurations of ϵ_i. We have to stress that n_q is a macroscopic operator (not a local one), and in the following analysis we study only such quantities. This implies that dynamical correlations functions, as defined by Eq. (3), are expected to be self-averaging, i.e., the configuration averaging is in principle not required in the macroscopic limit of $L \to \infty$. Here, we rely on a similarity with the treatment of Anderson localization of noninteracting (NI) electrons [31,32], as well on recent analysis of sample-to-sample fluctuations of $\sigma(\omega)$ in the same MBL model [12]. Nevertheless, this aspect still has to be critically examined when taking the limit $\omega \to 0$ since the fluctuations at larger disorder can be singular (referred to in 1D as the Griffiths effect of rare but large random deviations [8,9,33]). In particular, this is the relevant question within the nonergodic (MBL) phase.

The advantage of the above formulations is that it remains meaningful even in nonergodic cases where $\chi^0(q) > \chi(q,\omega \to 0)$ [31,32,34,35], as expected within the MBL regime. It is helpful to represent and analyze $\phi(q,\omega)$ in terms of complex memory functions [36] (see formal derivation and relations in Appendix B),

$$\phi(q,\omega) = \frac{-\chi^0(q)}{\omega + M(q,\omega)},$$
$$M(q,\omega) = \imath\frac{g_q^2}{\chi^0(q)}\sigma(q,\omega), \tag{4}$$

related to the q-dependent conductivity $\sigma(q,\omega)$ via the continuity equation $[H,n_q] = g_q j_q$, where $g_q = 2\sin(q/2)$ and j_q is the current operator for given q. It should be noted that $\sigma(q,\omega)$ has the usual meaning only in the limit $q \to 0$, where $\sigma(\omega) = \text{Re}\,\sigma(q \to 0,\omega)$ is the optical conductivity. We make a further step and define the current relaxation-rate function $\Gamma(q,\omega)$ as

$$\sigma(q,\omega) = \frac{\imath\chi_j^0(q)}{\omega + \Gamma(q,\omega)}, \tag{5}$$

where $\chi_j^0(q)$ is the static current susceptibility. We note that $\gamma(q,\omega) = \text{Im}\,\Gamma(q,\omega)$ is (at $\beta \to 0$) independent of β and has the meaning of the effective current relaxation rate at $\omega \to 0$.

The limit $\beta \to 0$ allows also for analytical evaluation of static quantities, in particular,

$$\chi^0(q) = \beta\bar{n}(1-\bar{n}) = \chi^0,$$
$$\chi_j^0(q) = \beta 2t^2\bar{n}(1-\bar{n}) = \chi_j^0. \tag{6}$$

With known static quantities [Eq. (6)], the relation between $\phi(q,\omega)$ and, e.g., $\Gamma(q,\omega)$ is thus unique and exact (not depending on approximations introduced later) and can be used in any direction provided that one of both quantities is evaluated. It is worth mentioning that Eq. (4) together with Eq. (5) resemble a continued fraction expansion of frequency moments of complex correlation functions. Such an approach was recently used in Ref. [37] to numerically evaluate optical conductivity $\sigma(\omega)$ in a strong disorder limit. Here, we develop analytical theory for the first three moments of such a series (see Sec. IV).

III. NUMERICAL FINITE-SIZE RESULTS

We note the relation of the above quantities to the standard dynamical structure factor $S(q,\omega)$, which is at $\beta \to 0$ given by

$$\text{Im}\,\phi(q,\omega) = \pi\beta S(q,\omega). \tag{7}$$

Before introducing the analytical method, we comment on numerical finite-size results, which serve later as a test for the proposed analytical theory. The dynamical quantity calculated directly is $S(q,\omega)$, whereby we employ the microcanonical Lanczos method (MCLM) on finite systems at $\beta \to 0$ [38,39]. In Fig. 1 we present characteristic results for $S(q,\omega)$ for $L = 24$, $V = 1$, $W = 0,2,4$ in the whole range of wave vectors $q = [0,\pi]$. They already allow for some rough distinction of dynamical density correlations in three regimes: (a) at $W = 0$ $S(q,\omega)$ is the response of the homogeneous 1D chain of interacting spinless fermions. Due to integrability of such a model, even at $\beta \to 0$ the response has a close analogy to NI fermions (i.e., at $V = 0$) [40]. In particular, the $S(q,\omega)$ has no diffusion pole and is quite featureless (at $\beta \to 0$) in the interval $\omega < 4\sin(q/2)$. (b) At weak disorder $0 < W = 2 < W_c \approx 3.5$ [10] an additional feature is a diffusion (or diffusionlike, as discussed later in relation to subdiffusion) pole which has a finite width $\delta\omega \propto q^2$ and is well visible at small $q \ll \pi/2$. (c) For large disorder $W = 4 > W_c$ the response becomes singular at all q and $S(q,\omega \approx 0) = S_q\delta(\omega)$ shows a finite stiffness $S_q > 0$, being a hallmark of the MBL regime.

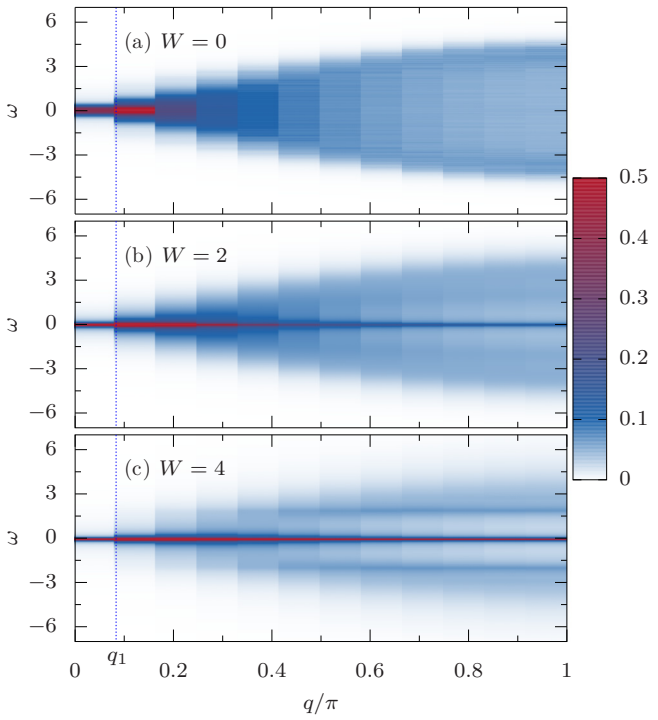

FIG. 1. High-temperature $\beta \to 0$ dynamical structure factor $S(q,\omega)$ as calculated with MCLM for $L = 24$, $V = 1$, (a) $W = 0$, (b) $W = 2$, and (c) $W = 4$ for all $q = [0,\pi]$.

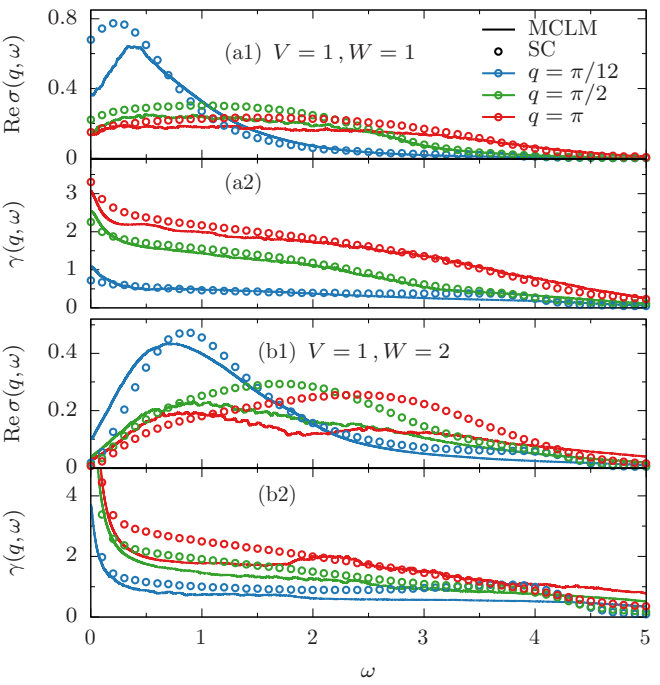

FIG. 2. (a1), (b1), (c1) Dynamical conductivity $\mathrm{Re}\,\sigma(q,\omega)$ and (a2), (b2), (c2) current relaxation-rate function $\gamma(q,\omega)$, obtained via MCLM on $L = 24$ sites for fixed parameters $V = 1$, as compared to the solution of SC equations (with effective length $L^* = 24$) for different q and two disorders: (a) $W = 1$ and (b) $W = 2$.

Since $S(q,\omega)$ is a quite singular function (at least for $q \to 0$), it is helpful to extract the corresponding $\sigma(q,\omega)$ and $\Gamma(q,\omega)$ via Eqs. (4) and (5). To this purpose we first calculate complex $\phi(q,\omega)$ from $S(q,\omega)$. Next, with known χ^0, χ^0_j using Eqs. (4) and (5) we evaluate $\sigma(q,\omega)$ and $\Gamma(q,\omega)$. In the numerical procedure it is crucial to have high-frequency ω resolution of MCLM results, which are obtained by employing $N_L \approx 10^4$ Lanczos steps in order to get $\delta\omega \lesssim 0.003$ of $S(q,\omega)$ spectra.

Characteristic results obtained for $L = 24$ and averaged over $N_s \approx 100$ random configurations are presented in Fig. 2. Some generic features be inferred: (a) Consistent with previous calculations of $\sigma(\omega)$ [7,9,11,12] our results indicate (for all disorders W) the maximum at $\omega = \omega^* > 0$, and more important, a nonanalytical low-ω behavior, i.e., $\sigma(\omega) \approx \sigma_0 + \zeta|\omega|^\alpha$. Here our numerical results in the ergodic regime, $W < W_c$, imply an interpretation with $\sigma_0 > 0$ and $\alpha \approx 1$ [7,11,12], while we comment later on the possibility of the subdiffusion with $\sigma_0 = 0$ and $\alpha < 1$ [8,9,24,26]. (b) Within our resolution σ_0, but also general $\sigma(q,\omega \to 0)$, vanishes for $W \geqslant W_c$, consistent with the onset of the MBL phase and nonergodicity at all q. This implies necessarily via Eq. (5) a divergent $\gamma(q,\omega \to 0) \to \infty$, as also evident on approaching the MBL transition.

For comparison we present in Fig. 3 also corresponding numerical results for $V = 2$, which corresponds to the isotropic Heisenberg model with random magnetic fields and has been in this connection studied more frequently. One can notice that larger V does not change qualitatively results for both $\sigma(q,\omega)$ as well as $\gamma(q,\omega)$, but rather additionally broadens spectra, except the MBL singularity at $\omega \approx 0$ for $W = 2$.

IV. ANALYTICAL APPROACH TO CURRENT-DECAY-RATE FUNCTION

A. Effective force

The motivation for following an analytical approach and approximations comes form the perturbation theory, which can be performed for weak disorder $W \to 0$ (and somewhat more delicate for $V \to 0$) on the level of the current-decay-rate function $\Gamma(q,\omega)$, in analogy to the theory of current scattering mechanisms in simple metals [41]. Such a theory has been extended to the nontrivial problem of Anderson localization by taking it beyond the perturbative approximation [31,32,35], and we will partly follow an analogous treatment for the MBL problem.

The expression for $\Gamma(q,\omega)$ [see the formal derivation and Eq. (B7) in the Appendix B] is the starting point for the analytical approximations. The current scattering mechanism is determined by the operator for the effective force $F_q = Q\mathcal{L}j_q$, with the Liouville operator $\mathcal{L}j_q = [H, j_q]$ and Q representing the operator [36,42] which projects into space perpendicular to n_q (see Appendix B for details). $\mathcal{L}j_q$ can be evaluated explicitly from the model (1),

$$\mathcal{L}j_q = tg_q h^d_q - \frac{1}{\sqrt{L}}\sum_k g_k \epsilon_k h^k_{q-k} - \frac{V}{\sqrt{L}}\sum_k w_k n_k h^k_{q-k} + 2t^2 g_q n_q, \tag{8}$$

where $w_k = 2\sin(3k/2)$ and we define also (Fourier transforms of) kinetic energy, potential, and next-nearest hopping

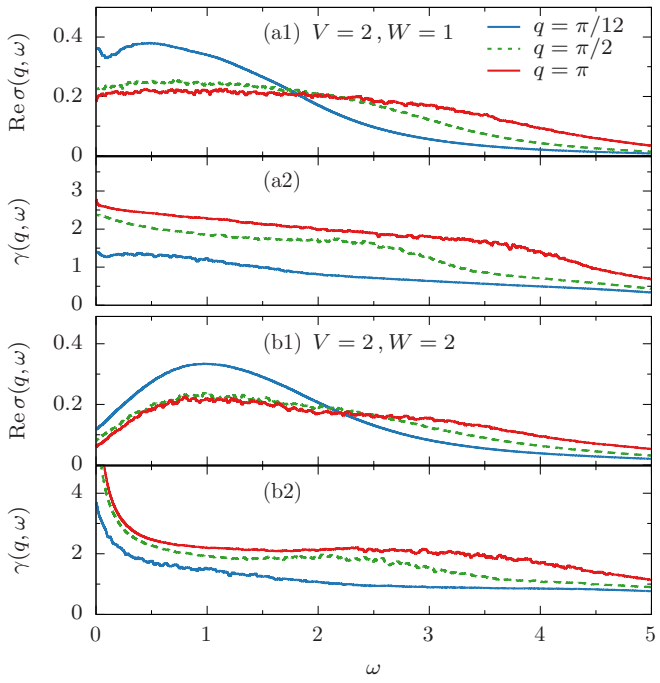

FIG. 3. (a1), (b1) $\mathrm{Re}\,\sigma(q,\omega)$ and (a2, b2) $\gamma(q,\omega)$ (MCLM, $L=24$) for fixed $V=2$, few different q, and two disorders: (a) $W=1$ and (b) $W=2$.

terms, respectively:

$$h_q^k = -\frac{t}{\sqrt{L}}\sum_i e^{\imath q(i+1/2)}[c_{i+1}^\dagger c_i + \mathrm{H.c.}],$$

$$h_q^d = -\frac{t}{\sqrt{L}}\sum_i e^{\imath qi}[c_{i+1}^\dagger c_{i-1} + \mathrm{H.c.}],$$

$$\epsilon_k = \frac{1}{\sqrt{L}}\sum_i e^{\imath qi}\epsilon_i. \tag{9}$$

In the evaluation of F_q the last term in Eq. (8) vanishes due to $Qn_q = 0$. The other three terms remain unaffected by the action of Q within the $\beta \to 0$ limit. With such a force operator F_q we can write

$$\Gamma(q,\omega) = \frac{1}{\chi_j^0}\Lambda(q,\omega),$$

$$\Lambda(q,\omega) \approx \frac{\chi_F(q,\omega) - \chi_F^0(q)}{\omega}, \tag{10}$$

where $\chi_F(q,\omega)$ are the generalized (force) susceptibilities, defined for the operator F_q [compare with Eq. (3)]. In the above expression, in analogy to weak scattering theory [36,41], we have introduced the (straightforward with a perturbative approach) approximation neglecting the projections onto n_q and j_q space, $\mathcal{L}_{QQ'} \to \mathcal{L}$, in the resolvent of Eq. (10) [compare Eq. (B7)].

B. Perturbative approximation

Following Eq. (B8) in Appendix B, we are dealing with force $F_q = F_{q1} + F_{q2} + F_{q3}$, representing different current scattering mechanisms. Similarly as in the derivation of the dynamical conductivity in metals [41], we represent $\Gamma(q,\omega)$ as the sum of three contributions, neglecting possible mixed correlations.

$\Lambda_1(q,\omega) \propto g_q^2$ vanishes in the hydrodynamic regime $q \to 0$ and can be approximated by the NI limit, i.e.,

$$\Gamma_1(q,\omega) = \frac{g_q^2}{2}\frac{1}{L}\sum_k \frac{-f_k^2}{\omega^+ + e_{k+q/2} - e_{k-q/2}}, \tag{11}$$

where $f_k = e_{2k}$ and $e_k = -2t\cos k$ is the NI fermion dispersion. It should be recognized, however, that even at $W = V = 0$ the $\Gamma_1(q,\omega)$ does not fully reproduce the NI result for $\phi(q,\omega)$ [due to simplification of the Liouville operator in Eqs. (B7) and (10)]. This deficiency is easily remedied by noticing that the correct NI result is obtained by replacing $f_k = e_k$ in Eq. (11). Still, for $W > 0$ single-particle eigenstates do not have a well-defined wave vector k, so a more reasonable approximation in this case is to assume an additional broadening, i.e., $\delta = W/\sqrt{3}$, corresponding to the width of the random-potential distribution. These details hardly influence any qualitative results further, since $\Gamma_1(q,\omega)$ does not contribute in the hydrodynamic regime $q \to 0$.

By decoupling the static disorder and dynamical density fluctuations in $\Gamma_2(q,\omega)$, we get

$$\Lambda_2(q,\omega) = \frac{1}{L}\sum_k g_{q-k}^2\langle\epsilon_{q-k}^2\rangle\phi_k(k,\omega), \tag{12}$$

where $\phi_k(q)$ is the relaxation function of the kinetic energy h_q^k [Eq. (9)], defined in analogy to $\phi(q,\omega)$ [Eq. (3)]. In the NI limit (but with disorder $W > 0$) Eq. (12) reduces to

$$\Gamma_2(q,\omega) = \frac{W^2}{6t^2L^2}\sum_{k,k'} \frac{-g_{q-k}^2 e_{k'}^2}{\omega^+ + e_{k'+k/2} - e_{k'-k/2}}, \tag{13}$$

which is the lowest-order scattering (Boltzmann-type) result [41]; in particular, it gives a finite relaxation rate $\gamma(q,\omega) = \mathrm{Im}\,\Gamma(q,\omega)$, also in the hydrodynamic $(q,\omega) \to 0$ limit.

The perturbative treatment of the interaction term is more problematic. One can assume that the dynamical fluctuations of density n_k and kinetic energy h_{q-k}^k are independent, which leads to

$$\mathrm{Im}\,\Lambda_3(q,\omega) = \frac{V^2}{L}\sum_k \frac{w_k^2}{\pi\beta}\int_{-\infty}^{\infty} d\omega' \times \mathrm{Im}\,\phi(k,\omega')\mathrm{Im}\,\phi_k(q-k,\omega-\omega'). \tag{14}$$

When we insert the NI input for $\phi(q,\omega)$ and $\phi_k(q,\omega)$, the interaction $V > 0$ leads to an additional current-decay channel, even at $(q,\omega) \to 0$. While this is an effect generally expected from the interparticle interaction, in our particular case it is not fully justified since the pure ($W = 0$) model is integrable and exhibits a dissipationless current and singular $\sigma(\omega \approx 0) = \beta D\delta(\omega)$ with $D > 0$ even at $\beta \to 0$. Since we are interested more in the role of disorder and in a generic interaction term, where current dissipation should emerge from a term like Eq. (14), we would here stay at this level of approximation.

C. Self-consistent closure

At this stage we are not aiming to develop a more detailed theory for kinetic-energy fluctuations $\phi_k(q,\omega)$

entering Eqs. (13) and (14). It is, however, crucial to take into account the fact that the kinetic-energy function has an overlap with the energy-density relaxation function. In a disordered system, the energy is, besides the number of particles, the only conserved quantity. It is therefore essential to take properly the $q \to 0$ energy fluctuations, and we treat these correlations in analogy to Eqs. (4) and (5) with the role of $\sigma(q,\omega)$ replaced by the thermal conductivity $\kappa(q,\omega)$. The latter has been found [43,44] to have similar behavior close to the MBL transition, in particular, the vanishing of the dc value κ_0 and anomalous low-ω behavior. Taking into account the sum rules $\eta = \chi_k^0/\chi^0 = 2t^2$, we further work with a simplification $\phi_k(q,\omega) = \eta\phi(q,\omega)$ representing an effective Wiedemann-Franz relation, i.e., assuming the same relaxation rates for density and energy currents.

Since $\Lambda \propto \phi \propto \beta$, we now work with renormalized relaxation functions, i.e., $\widetilde{\phi} = \phi/\chi^0, \widetilde{\phi}_k = \phi_k/\chi^0$. So the final SC equations, besides $\Gamma_1(q,\omega)$, where we do not correct Eq. (11), are

$$\Gamma_2(q,\omega) = \frac{\eta W^2}{6t^2 L}\sum_k g_{q-k}^2 \widetilde{\phi}(k,\omega), \tag{15}$$

$$\mathrm{Im}\,\Gamma_3(q,\omega) = \frac{\eta\widetilde{n}V^2}{2\pi L}\sum_k w_k^2 \int d\omega'\,\mathrm{Im}\,\widetilde{\phi}(k,\omega') \times \mathrm{Im}\,\widetilde{\phi}(q-k,\omega-\omega'), \tag{16}$$

where $\widetilde{n} = \bar{n}(1-\bar{n})$. The MBL physics, in particular the transition, is predominantly governed by $\Gamma_2(q,\omega)$, while for $W > 0$ the interaction-driven term $\Gamma_3(q,\omega)$, due to convolutions in (q,ω), yields rather a featureless function, leading to the current decay at all q.

Due to the coupling to the $q \to 0$ diffusion mode in Eq. (11), it is evident that $\Gamma(q,\omega \to 0)$ as well as the whole SC set might be singular in 1D. In order to simulate finite-size systems (as studied numerically) and explore the finite-size scaling we introduce a finite cutoff $k_m = \pi/L^*$, in particular in Eq. (15). It should be noted that after taking the mentioned simplifications there are (at given model constants V,W) no free parameters in the SC theory apart from the cutoff k_m (effective length L^*).

We note that the presented SC equations have an analogy to simplified theories of Anderson localization [35]. It has been, however, established that proper SC localization theory for NI fermions [31,32] should take into account the time-reversal symmetry of correlation functions on a single-particle level. The latter is, however, lost by including finite interaction $V > 0$. As a consequence, Eq. (15) emerges as a nontrivial coupling of the only remaining low-ω collective modes in the system, i.e., the density and the energy diffusion mode.

V. NUMERICAL SOLUTIONS OF SC EQUATIONS

A. General features

Having a SC set of equations, Eqs. (4), (5), (11), (15), and (16), it is straightforward to find solutions by numerical iteration of coupled equations until convergence, whereby we use at the initial step the NI input for $\phi(q,\omega)$. In Fig. 2 we present typical SC-theory results for $\mathrm{Re}\,\sigma(q,\omega)$ and $\gamma(q,\omega)$

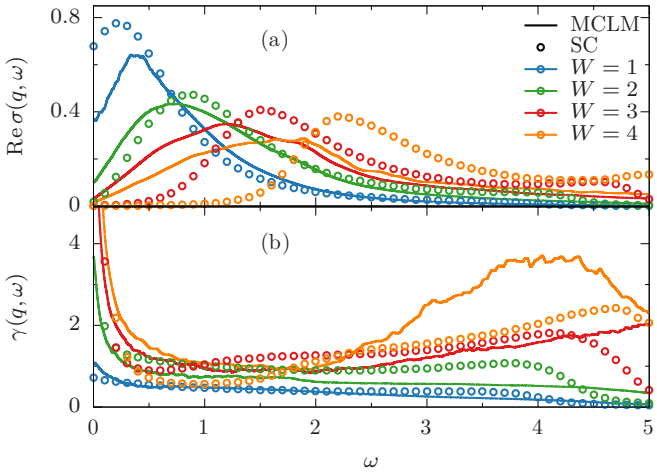

FIG. 4. Comparison between SC and numerical (MCLM) results of (a) $\mathrm{Re}\sigma(q,\omega)$ and (b) $\gamma(q,\omega)$ for $q = \pi/12$, $L = L^* = 24$, and various disorder strengths $W = 1,2,3,4$.

along with the MCLM numerical ones, whereby we use $L^* = 24$ corresponding to the size used in MCLM calculation. Qualitative agreement is quite satisfactory for a modest value of disorder strength W, in particular, the analytical theory reproduces some essential features: (a) A maxima of $\sigma(q,\omega)$ with $\omega^* > 0$ emerges also in SC solutions due to a nontrivial maxima in $\gamma(q,\omega \to 0)$. The maximum moves towards $\omega^* \approx 0$ for weaker disorder $W < 0.8$, which would be the signature of a normal diffusion. (b) In the ergodic regime at $W < W_c^* \approx 1.6$, low-ω SC results for small $L^* < 100$ can be roughly fitted to $\sigma(\omega) = \sigma_0 + b|\omega|^\alpha$, with $\sigma_0 > 0$ and $\alpha \approx 1$ close to the MBL transition. (c) Due to a large increase of $\gamma(q,\omega \to 0)$ the conductivity $\sigma(q,\omega \to 0)$ is strongly reduced for larger $W > 1$. (d) Eventually, for $W > W_c^*$ the SC equations yield a singular solution $\gamma(q,\omega \approx 0) = \gamma_s\delta(\omega)$, which is the hallmark of the nonergodicity and leads also to vanishing dc transport $\sigma(q,\omega \to 0) = 0$.

The behavior with W varying across the MBL transition is presented in Fig. 4, where we compare results for disorder strength up to $W = 4 \gg W_c^*$. We observe that the quantitative agreement between SC and the numerical result is steadily decreasing with increasing $W > W_c^*$. This coincides with the fact that the SC threshold $W_c^* \approx 1.6$ is significantly below the numerical (at $V = 1$) estimate $W_c \approx 3$ [10]. The origin of this discrepancy in critical W_c^* can be traced back to overestimated coupling between density and the energy diffusion mode enhancing the feedback (localization) mechanism in SC equations via the $\gamma(q,\omega \to 0)$ behavior. Still, the overall qualitative change across the MBL transition follows the same pattern as the numerical one.

When we are comparing SC results for optical conductivity $\sigma(\omega) = \sigma(q \to 0,\omega)$ with previous numerical studies (as well as this study for $q > 0$) on finite systems [11,12,43], we should use appropriate L^* as well as corresponding $\delta\omega$. In Fig. 5 we present a characteristic result for modest $L^* = 40$ (and $\delta\omega \approx 10^{-3}$) for $\sigma(\omega)$ across the transition to the MBL, i.e., $1.2 \leqslant W \leqslant 2.0$, together with the low-$\omega$ fit to $\tilde{\sigma}(\omega) = a + b|\omega|^c$. We note that such a fit should be evidently restricted to the range well below the maximum $\omega \ll \omega^*$ which is for $W > W_c^*$ at

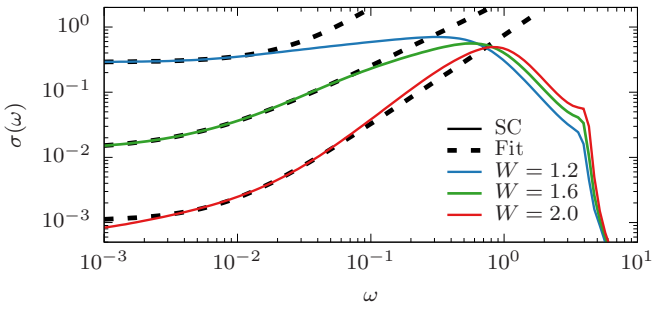

FIG. 5. Comparison of SC solution (solid line, $L^* = 40$, $\delta\omega = 10^{-3}$) with the fit $\tilde{\sigma}(\omega) = a + b|\omega|^c$ (dashed line) with $c = 0.8, 1.0, 1.5$ for $W = 1.2, 1.6, 2.0$, respectively.

$\omega^* \approx 1$, but for the lowest $W = 1.2$ moves down to $\omega^* \approx 0.2$ [11]. Nevertheless, the overall behavior around the transition $W \approx W_c^*$ is is characterized by $\alpha \approx 1$ and a clear drop of σ_0.

B. Subdiffusion and transition to MBL

While SC results in Fig. 2 (as well as Fig. 5) show an overall behavior for $W < W_c^*$ and $W \approx W_c^*$, consistent with numerical results at finite L^*, we further investigate in more detail the consequences of the singular aspects due to 1D. In order to explore the low-ω behavior, we concentrate on the most interesting $q \to 0$ results and present in Fig. 6 $\sigma(\omega)$ as obtained with large frequency ω resolution ($\delta\omega \approx 10^{-4}$) at several characteristic W and varying effective lengths $L^* = 20$–320. It should be realized that the choice of $\delta\omega$ in the numerical SC procedure is intimately related to L^* and we cannot get strictly $\sigma_0 = 0$ at $\delta\omega > 0$. Nevertheless, the scaling $\delta\omega \to 0$, as shown in the inset of Fig. 6, is consistent with vanishing $\sigma_0 = 0$, at least for $W > 1.2$. This is also presented in Fig. 7, which depicts the dependence of dynamical

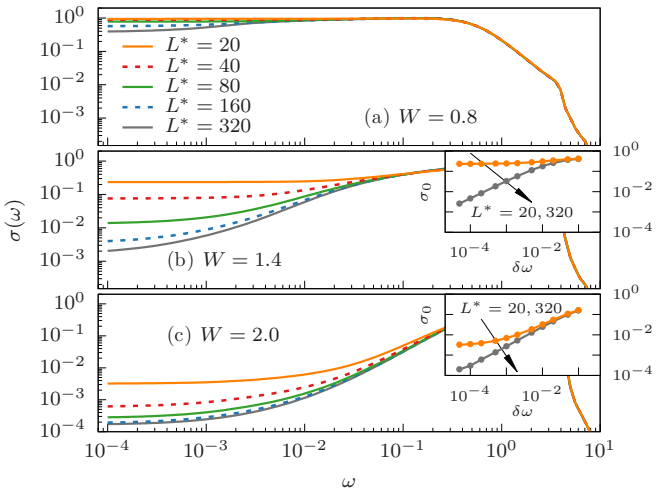

FIG. 6. Optical conductivity $\sigma(\omega)$ (in a log-log scale) as evaluated from the SC theory at $V = 1$ for different $W = 0.8, 1.4, 2.0$, and various effective lengths $L^* = 20$–320 with frequency resolution $\delta\omega = 10^{-4}$. Insets of (b,c): scaling of $L^* = 20$ and $L^* = 320$ with $\delta\omega$ used in SC equations.

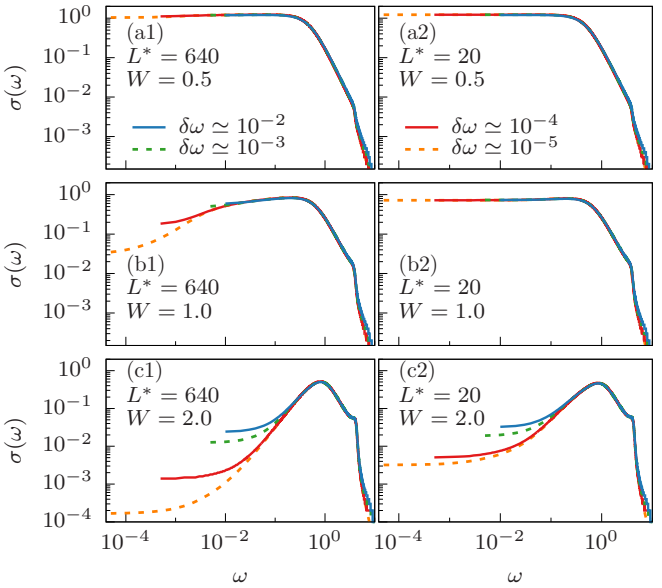

FIG. 7. (a)–(c) Frequency resolution $\delta\omega$ dependence of $\sigma(\omega)$ for fixed effective lengths $L^* = 640$ (left column) and $L^* = 20$ (right column), and various disorder strengths $W = 0.5, 1.0, 2.0$.

conductivity $\mathrm{Re}\,\sigma(q,\omega)$ on frequency resolution $\delta\omega$ for fixed cutoff $L^* = 20$ and $L^* = 640$ and various disorder strengths.

Taking this into account, we can distinguish three regimes as already noted in numerical studies [8,9,26]: (a) At small disorder $W < 1$ $\sigma(\omega \to 0)$ is only weakly dependent on L^*, and it is hard to detect signatures of a subdiffusion even at extreme $L^* \gg 100$. (b) At the intermediate $1 < W < W_c^*$ we confirm the steady decrease of σ_0 with increasing L^*, and the behavior can be well captured with subdiffusion form $\sigma(\omega) \propto |\omega|^\alpha$ with $\alpha < 1$. (c) For $W > W_c^*$ results become again only weakly L^* dependent, while the dc value σ_0 is vanishing.

To make the analysis of subdiffusion more objective, we define the exponent via the maximum slope

$$\alpha = \frac{d\,\log\sigma(\omega)}{d\,\log\omega} \tag{17}$$

in the range $\omega < 0.1$. Results are shown in Fig. 8(a). It is indicative that the subdiffusion with $\alpha \ll 1$ can be hardly established for $W < 1$ since it requires $L^* \gg 100$ [26]. On the other hand, results with $\alpha > 0.3$ are better resolved. The crossing $\alpha = 1$ marks the MBL transition to the nonergodic phase, where for large $W \gg W_c^*$ we get $\alpha \approx 2$, as expected deep inside the localized regime [2].

As a uniform ($q \to 0$) order parameter within the MBL (nonergodic) phase one can consider the current-relaxation stiffness $\gamma_s(q) > 0$. More physical is the dielectric polarizability

$$\chi_d = \frac{2}{\pi}\int_0^\infty \frac{\sigma(\omega)}{\omega^2} d\omega, \tag{18}$$

whereby $\chi_d < \infty$ implies that the system is dielectric, i.e., an external field along the chain induces only a finite polarization. It is evident that $\alpha > 1$ is required for $\chi_d < \infty$. In Fig. 8(b) we present results for the inverse $1/\chi_d$ vs W as evaluated for

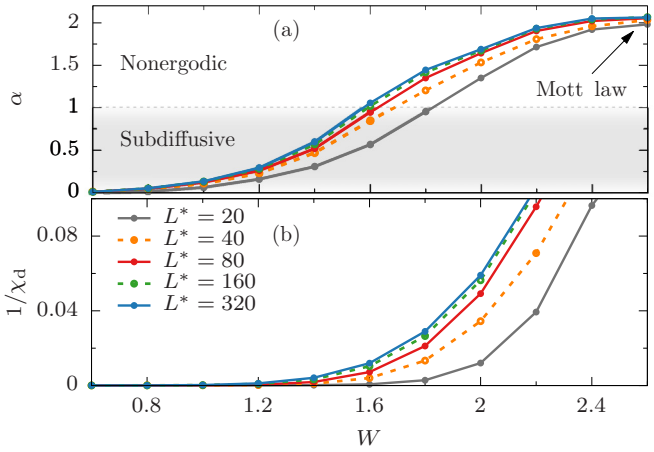

FIG. 8. (a) Dynamical exponent α and (b) the inverse dielectric polarizability $1/\chi_d$ vs W as evaluated at $V = 1$ and different $L^* =$ 20–320 and $\delta\omega = 10^{-4}$. Note that the MBL transition is determined by $\alpha = 1$.

different L^*, revealing indeed its vanishing below the MBL transition.

VI. CONCLUSIONS

The presented analytical theory is a SC extension of the perturbative evaluation of the current-decay-rate function $\Gamma(q,\omega)$. The disorder effect is reproduced within the lowest order (Boltzmann-type) scattering, while the interaction is treated only within a decoupling approximation. In analogy to the SC theory of the single-particle Anderson localization [31,32,35], the theory is closed beyond the weak scattering approximation, where the crucial assumption (at the present level of the theory) is that density and energy dynamical correlations are related, in particular at small (q,ω), and both simultaneously undergo a MBL transition.

Although the theory starts from the lowest-order calculation of the current-relaxation function $\Gamma(q,\omega)$ its extension into a SC scheme goes well beyond the perturbative approach. A SC determination of $\Gamma(q,\omega)$ leads, on approaching the MBL transition, to enhanced low-ω density and energy-density fluctuations, which finally lead to the freezing of the low-ω dynamics at the $W = W_c^*$. Beyond this disorder correlation functions are nonergodic and characterized by a singular contribution in $S(q,\omega) \approx S_q\delta(\omega)$ with $S_q > 0$. One might question the particular validity and the form of the SC loop; however, the freezing of low-ω dynamics is well visible in the numerical results and consistent with analogous phenomenon in the theory of Anderson localization [31,32,35].

In the presented theory there are no free parameters except the cutoff $k_m = \pi/L^*$, which simulates the finite-size system and allows for the finite-size scaling. The importance of cutoff and corresponding sensitivity of SC solutions on the frequency resolution $\delta\omega$ appears to be a singular property of 1D and makes the proper convergence of solutions of coupled analytical equations nontrivial. In spite of simplifications, the presented SC theory yields several nontrivial conclusions, consistent with numerical results obtained in this paper via the MCLM method but also with previous numerical investigations on finite systems:

(a) When simulating numerically reachable finite-size systems by taking the cutoff $L^* \approx 20$–40 (as well as the corresponding finite-frequency resolution $\delta\omega \approx 10^{-3}$), our SC results appear to be consistent with the dynamical conductivity $\sigma(\omega) \approx \sigma_0 + b|\omega|^\alpha$ with $\alpha \approx 1$ and vanishing σ_0 near the MBL transition [11,12,43].

(b) However, careful scaling beyond $L^* > 100$ and $\delta\omega \ll 10^3$ of SC solution indicates on vanishing $\sigma_0 = 0$ in the ergodic regime $W < W_c^*$ (at least for $W > 1.2$ at $V = 1$). Within the present SC theory this emerges due to the disorder-induced coupling between the density and the energy diffusion mode. As a consequence of 1D, in the ergodic regime the transport is subdiffusive [8,9,24,25,27], i.e., for large enough systems dc transport coefficients are expected to vanish, e.g., $\sigma_0 \to 0$. Still, for modest disorder W effective sizes to detect such anomalies could be huge, e.g., $L^* \gg 100$ [26,27], and therefore hard to detect in numerical and even experimental studies.

(c) The transition to the nonergodic MBL regime $W > W_c$ appears in the theory via the onset of the current-decay stiffness $\gamma_s > 0$, which coincides with the condition for the dynamical exponent $\alpha > 1$ and the dielectric polarizability $\chi_d < \infty$.

(d) Theoretical results for dynamical correlations show an overall qualitative agreement with numerical ones (at corresponding effective length L^*) in the whole (q,ω) range.

When we discuss the validity and restrictions within the presented theory, there are several aspects in which should be considered:

(a) Since the theory is an extension of the perturbative treatment of disorder starting at modest W, it is plausible that we cannot claim a quantitative agreement for larger disorder with $W \approx W_c^*$ or even more within the MBL regime $W > W_c^*$. The reason is mainly twofold: At $W > 3$ single-particle states are already well localized. Still, more problematic seems to be the overestimated coupling between density and energy diffusion modes, which leads to overestimated feedback in SC equations and consequently to the transition at critical W_c^* being substantially smaller than emerging from numerical studies (e.g., at $V = 1$ $W_c^* \approx 1.6$ instead of the numerical estimate $W_c = 3$). This can be improved by taking both relevant hydrodynamic modes, i.e., density and energy diffusion, on an equal footing into the analysis. In this work we skip this aspect in order to make our SC theory as transparent as possible.

(b) The current-decay rate due to interaction $V > 0$ is taken very crudely, in particular since the actual model without disorder (at $W = 0$) is integrable and $V > 0$ itself does lead to dc conductivity $\sigma_0 < \infty$. Nevertheless, a generic interaction term is expected to lead to the scattering of dc current (at $T \gg 0$). Moreover, $\Gamma_3(q,\omega)$ seems to be less critically dependent on the dimensionality of the system, as appears to be the case for $\Gamma_2(q,\omega)$ emerging from disorder.

(c) The assumption that the dynamical quantities are self-averaging is inherent in the SC approach, although this aspect should be further critically examined due to possible role of rare large disorder fluctuations [8,9].

The presented SC scheme is more generic and can be generalized into different directions. Analogous treatment of higher dimension is rather straightforward, especially since

some anomalies such as, e.g., the subdiffusion are not expected there, at least not to such extent. One could treat also separately the density and energy dynamical correlations, whereby the latter are much less investigated so far. On the other hand, for experiments on MBL in cold-atom systems [22–24] the relevant model is the disordered Hubbard model, which does reveal a disorder-induced spin-charge separation [45], which might also be approached in a similar way.

ACKNOWLEDGMENTS

P.P. acknowledges support from program P1-0044 of the Slovenian Research Agency. J.H. acknowledges support by the US Department of Energy, Office of Basic Energy Sciences, Materials Science and Engineering Division.

APPENDIX A: CORRELATION FUNCTIONS

Since the system under consideration can be nonergodic, one should be careful with the definitions of correlation and response functions. In our analysis we define the dynamical susceptibility (response functions) $\chi_A(\omega)$ and corresponding static (thermodynamic) response χ_A^0 for arbitrary operators A in the standard way,

$$\chi_A(\omega) = -\imath \int_0^\infty dt\, \mathrm{e}^{i\omega^+ t} \langle [A^\dagger(t), A] \rangle, \tag{A1}$$

$$\chi_A^0 = \int_0^\beta d\tau\, \langle A^\dagger A(i\tau) \rangle = (A|A), \tag{A2}$$

where $\omega^+ = \omega + i\delta$ with $\delta \to 0$ and $\beta = 1/T$. Equation (A2) introduces the scalar product [36,42], convenient for formal representation and derivation of memory functions, even for nonergodic systems. Above $\langle .. \rangle$ denotes the canonical thermodynamical average and in a disordered system additional averaging over all random configurations of ϵ_i [see the comment in the main text after Eq. (3)].

In the analysis, instead of susceptibilities $\chi_A(\omega)$, we mostly use related relaxation functions,

$$\phi_A(\omega) = \frac{\chi_A(\omega) - \chi_A^0}{\omega} = \left(A \left| \frac{1}{\mathcal{L} - \omega} \right| A \right), \tag{A3}$$

where the second representation in Eq. (A3) in terms of the resolvent with Liouville operator $\mathcal{L}A = [H, A]$ is a standard one allowing formal steps further-on. The nonergodic behavior is in this framework characterized by the behavior $\chi_A^0 > \chi_A(\omega \to 0)$, leading to a singular low-ω contribution [31,32,34,35],

$$\mathrm{Im}\, \phi_A(\omega \sim 0) = \pi D_A \delta(\omega), \quad D_A = \chi_A^0 - \chi_A(\omega \to 0), \tag{A4}$$

where D_A is the corresponding stiffness.

Finally, since we are dealing only with the case of high T, i.e., $\beta \to 0$, there are convenient simplifications following from Eqs. (A2) and (A3),

$$\chi_A^0 = \beta \langle A^\dagger A \rangle, \quad \phi_A(\omega) = -\imath\beta \int_0^\infty dt\, \mathrm{e}^{\imath\omega^+ t} \langle A^\dagger(t) A \rangle, \tag{A5}$$

and in particular, a simplified relation to the general dynamical structure factor $\mathrm{Im}\, \phi(\omega) = \pi\beta S_A(\omega)$.

APPENDIX B: MEMORY-FUNCTION REPRESENTATION

We use the definitions above for several operators A of interest. The starting point is the density relaxation function with $A = n_q$. The memory-function (MF) representation of $\phi(q,\omega)$ follows from the continuity equation,

$$\mathcal{L} n_q = g_q j_q, \quad j_q = \frac{t}{\sqrt{L}} \sum_i \mathrm{e}^{\imath q(i+1/2)} (\imath c_{i+1}^\dagger c_i + \mathrm{H.c.}), \tag{B1}$$

where $g_q = 2\sin(q/2)$. By defining the projection projector P and its complement Q,

$$P = |n_q) \frac{1}{\chi^0(q)} (n_q|, \quad Q = 1 - P, \tag{B2}$$

where $\chi^0(q) = (n_q|n_q)$, we can express relaxation function, Eq. (A3), in the form of MF representation,

$$\phi(q,\omega) = \frac{-\chi^0(q)}{\omega + \imath g_q^2 \sigma(q,\omega)/\chi^0(q)}, \tag{B3}$$

with

$$\sigma(q,\omega) = \left(Qj_q \left| \frac{-\imath}{\mathcal{L}_Q - \omega} \right| Qj_q \right) = \left(j_q \left| \frac{-\imath}{\mathcal{L}_Q - \omega} \right| j_q \right), \tag{B4}$$

where $\mathcal{L}_Q = Q\mathcal{L}Q$ is the projected Liouville operator and $Qj_q = j_q$ by symmetry. It should be noted that $\sigma(q,\omega)$ is in general not equal to standard conductivity $\tilde{\sigma}(q,\omega)$, evaluated directly by replacing the reduced dynamics in Eq. (B4) with the full one, $\mathcal{L}_Q \to \mathcal{L}$. Still, both quantities merge in the hydrodynamic limit $q \to 0$ [36,41].

In the next step we express $\sigma(q,\omega)$ in terms of the current relaxation-rate function $\Gamma(q,\omega)$,

$$\sigma(q,\omega) = \imath \frac{\chi_j^0(q)}{\omega + \Gamma(q,\omega)}, \tag{B5}$$

where $\chi_j^0(q) = (j_q|j_q)$. While such a possibility follows directly from the analytical properties of $\phi(q,\omega)$ and $\sigma(q,\omega)$, the formal expression (used further-on as the starting point for analytical approximations in Sec. IV) can be given, introducing an additional projector

$$P' = |j_q) \frac{1}{\chi^0(q)} (j_q|, \quad Q' = 1 - P', \tag{B6}$$

so that

$$\Gamma(q,\omega) = \frac{1}{\chi_j^0(q)} \left(F_q \left| \frac{1}{\mathcal{L}_{QQ'} - \omega} \right| F_q \right) = \frac{1}{\chi_j^0(q)} \Lambda(q,\omega), \tag{B7}$$

where (formally) $\mathcal{L}_{QQ'} = Q'\mathcal{L}_Q Q'$ and

$$F_q = QQ'\mathcal{L}j_q = Q\mathcal{L}j_q. \tag{B8}$$

[1] P. W. Anderson, Absence of diffusion in certain random lattices, Phys. Rev. **109**, 1492 (1958).

[2] N. F. Mott, Conduction in non-crystalline systems, Philos. Mag. (1798–1977) **17**, 1259 (1968).

[3] L. Fleishman and P. W. Anderson, Interactions and the Anderson transition, Phys. Rev. B **21**, 2366 (1980).

[4] D. M. Basko, I. L. Aleiner, and B. L. Altshuler, Metal–insulator transition in a weakly interacting many-electron system with localized single-particle states, Ann. Phys. (NY) **321**, 1126 (2006).

[5] V. Oganesyan and D. A. Huse, Localization of interacting fermions at high temperature, Phys. Rev. B **75**, 155111 (2007).

[6] T. C. Berkelbach and D. R. Reichman, Conductivity of disordered quantum lattice models at infinite temperature: Many-body localization, Phys. Rev. B **81**, 224429 (2010).

[7] O. S. Barišić and P. Prelovšek, Conductivity in a disordered one-dimensional system of interacting fermions, Phys. Rev. B **82**, 161106 (2010).

[8] K. Agarwal, S. Gopalakrishnan, M. Knap, M. Müller, and E. Demler, Anomalous Diffusion and Griffiths Effects Near the Many-Body Localization Transition, Phys. Rev. Lett. **114**, 160401 (2015).

[9] S. Gopalakrishnan, M. Müller, V. Khemani, M. Knap, E. Demler, and D. A. Huse, Low-frequency conductivity in many-body localized systems, Phys. Rev. B **92**, 104202 (2015).

[10] Y. Bar Lev, G. Cohen, and D. R. Reichman, Absence of Diffusion in an Interacting System of Spinless Fermions on a One-Dimensional Disordered Lattice, Phys. Rev. Lett. **114**, 100601 (2015).

[11] R. Steinigeweg, J. Herbrych, F. Pollmann, and W. Brenig, Typicality approach to the optical conductivity in thermal and many-body localized phases, Phys. Rev. B **94**, 180401(R) (2016).

[12] O. S. Barišić, J. Kokalj, I. Balog, and P. Prelovšek, Dynamical conductivity and its fluctuations along the crossover to many-body localization, Phys. Rev. B **94**, 045126 (2016).

[13] A. Pal and D. A. Huse, Many-body localization phase transition, Phys. Rev. B **82**, 174411 (2010).

[14] M. Serbyn, Z. Papić, and D. A. Abanin, Local Conservation Laws and the Structure of the Many-Body Localized States, Phys. Rev. Lett. **111**, 127201 (2013).

[15] A. De Luca and A. Scardicchio, Ergodicity breaking in a model showing many-body localization, Europhys. Lett. **101**, 37003 (2013).

[16] D. A. Huse, R. Nandkishore, and V. Oganesyan, Phenomenology of fully many-body-localized systems, Phys. Rev. B **90**, 174202 (2014).

[17] R. Vosk and E. Altman, Many-Body Localization in One Dimension as a Dynamical Renormalization Group Fixed Point, Phys. Rev. Lett. **110**, 067204 (2013).

[18] D. A. Huse, R. Nandkishore, V. Oganesyan, A. Pal, and S. L. Sondhi, Localization-protected quantum order, Phys. Rev. B **88**, 014206 (2013).

[19] M. Serbyn, Z. Papić, and D. A. Abanin, Quantum quenches in the many-body localized phase, Phys. Rev. B **90**, 174302 (2014).

[20] R. Vasseur, S. A. Parameswaran, and J. E. Moore, Quantum revivals and many-body localization, Phys. Rev. B **91**, 140202 (2015).

[21] S. S. Kondov, W. R. McGehee, W. Xu, and B. DeMarco, Disorder-Induced Localization in a Strongly Correlated Atomic Hubbard Gas, Phys. Rev. Lett. **114**, 083002 (2015).

[22] M. Schreiber, S. S. Hodgman, P. Bordia, H. P. Lüschen, M. H. Fischer, R. Vosk, E. Altman, U. Schneider, and I. Bloch, Observation of many-body localization of interacting fermions in a quasi-random optical lattice, Science **349**, 842 (2015).

[23] P. Bordia, H. P. Lüschen, S. S. Hodgman, M. Schreiber, I. Bloch, and U. Schneider, Coupling Identical 1D Many-Body Localized Systems, Phys. Rev. Lett. **116**, 140401 (2016).

[24] H. P. Lüschen, P. Bordia, S. Scherg, F. Alet, E. Altman, U. Schneider, and I. Bloch, Evidence for Griffiths-type dynamics near the many-body localization transition in quasi-periodic systems, arXiv:1612.07173.

[25] D. J. Luitz, N. Laflorencie, and F. Alet, Extended slow dynamical regime prefiguring the many-body localization transition, Phys. Rev. B **93**, 060201 (2016).

[26] M. Žnidarič, A. Scardicchio, and V. K. Varma, Diffusive and Subdiffusive Spin Transport in the Ergodic Phase of a Many-Body Localizable System, Phys. Rev. Lett. **117**, 040601 (2016).

[27] D. J. Luitz and Y. B. Lev, The ergodic side of the many-body localization transition, Ann. Phys. **529**, 1600350 (2017).

[28] R. Vosk, D. A. Huse, and E. Altman, Theory of the Many-Body Localization Transition in One-Dimensional Systems, Phys. Rev. X **5**, 031032 (2015).

[29] D. J. Luitz, N. Laflorencie, and F. Alet, Many-body localization edge in the random-field Heisenberg chain, Phys. Rev. B **91**, 081103 (2015).

[30] M. Mierzejewski, J. Herbrych, and P. Prelovšek, Universal dynamics of density correlations at the transition to a many-body localized state, Phys. Rev. B **94**, 224207 (2016).

[31] D. Vollhardt and P. Wölfle, Anderson Localization in $d <\sim 2$ Dimensions: A Self-Consistent Diagrammatic Theory, Phys. Rev. Lett. **45**, 842 (1980).

[32] D. Vollhardt and P. Wölfle, Diagrammatic, self-consistent treatment of the Anderson localization problem in $d \leqslant 2$ dimensions, Phys. Rev. B **22**, 4666 (1980).

[33] S. Gopalakrishnan, K. Agarwal, E. A. Demler, D. A. Huse, and M. Knap, Griffiths effects and slow dynamics in nearly many-body localized systems, Phys. Rev. B **93**, 134206 (2016).

[34] R. Pirc and G. Dick, Exact isolated and isothermal susceptibilities for an interacting dipole-lattice system, Phys. Rev. B **9**, 2701 (1974).

[35] W. Götze, Strong three-dimensional random potential, J. Phys. C: Solid State Phys. **12**, 1279 (1979).

[36] D. Forster, *Hydrodynamic Fluctuations, Broken Symmetry, and Correlation Functions* (Westview Press, New York, 1995).

[37] I. Khait, S. Gazit, N. Y. Yao, and A. Auerbach, Spin transport of weakly disordered Heisenberg chain at infinite temperature, Phys. Rev. B **93**, 224205 (2016).

[38] M. W. Long, P. Prelovšek, S. El Shawish, J. Karadamoglou, and X. Zotos, Finite-temperature dynamical correlations using the microcanonical ensemble and the Lanczos algorithm, Phys. Rev. B **68**, 235106 (2003).

[39] P. Prelovšek and J. Bonča, Ground state and finite temperature Lanczos methods, in *Strongly Correlated Systems–Numerical*

Methods, edited by A. Avella and F. Mancini (Springer, Berlin, 2013).

[40] J. Herbrych, R. Steinigeweg, and P. Prelovšek, Spin hydrodynamics in the $s = 1/2$ anisotropic Heisenberg chain, Phys. Rev. B **86**, 115106 (2012).

[41] W. Götze and P. Wölfle, Homogeneous dynamical conductivity of simple metals, Phys. Rev. B **6**, 1226 (1972).

[42] H. Mori, Transport, collective motion, and Brownian motion, Prog. Theor. Phys. **33**, 423 (1965).

[43] A. Karahalios, A. Metavitsiadis, X. Zotos, A. Gorczyca, and P. Prelovšek, Finite-temperature transport in disordered Heisenberg chains, Phys. Rev. B **79**, 024425 (2009).

[44] P. Prelovšek, M. Mierzejewski, O. Barišić, and J. Herbrych, Density correlations and transport in models of many-body localization, Ann. Phys. (Berlin) **529**, 1600362 (2017).

[45] P. Prelovšek, O. S. Barišić, and M. Žnidarič, Absence of full many-body localization in the disordered Hubbard chain, Phys. Rev. B **94**, 241104 (2016).